35th International Electric Vehicle Symposium and Exhibition (EVS35)
Oslo, Norway, June 11-15, 2022

Electromagnetic Environment Safety Evaluation of Wireless Power Transfer Systems for Electric Vehicles

Yang Yang[1], Jinlong Cui[1],Shengyue Dou[1], Abdelhak Marr[1],
Yuanfeng Lan[2,3],Mohamed El Baghdadi[2,3],Omar Hegazy[2,3]

[1]*School of Automobile, Chang'an University, Xi'an, China, yayang@chd.edu.cn*

[2]*Vrije Universiteit Brussel (VUB), ETEC Dept.*
& MOBI-EPOWERS Research
Group,1050 Brussel, Belgium

[3]*Flanders Make, Leuven 3001, Belgium*

Summary

To study and evaluate the electromagnetic radiation problems of the wireless charging system for electric vehicles, a circular coil was established to analyze the electromagnetic field distribution around the car body using finite element software COMSOL™. In this paper, an adult's height is designed according to Human Engineering especially for Chinese people and then the six organ models were established, representing sole, liver, spleen, heart, lung and kidney. Then the electromagnetic safety of the human body is analyzed under the different scenarios of only coils, coils with ferrite cores and coils with ferrite cores and aluminum plates at the resonant frequency of 85 kHz and the transmission power of 3.7 kW, respectively. This study indicates that electromagnetic safety indexes of each organ meet the International Commission on Non-Ionizing Radiation Protection (ICNIRP) standard. Besides, the maximum magnetic field intensity value of the sole is biggest which indicates that the feet should be prevented from touching the part of being close to a normally working WPT system.

Keywords: Wireless Power Transfer Systems, Inductive Charging, Electromagnetic Environment, Safety Evaluation, Electric Vehicles

1 Introduction

In recent years, wireless power transfer (WPT) technology has got more and more attention among car manufacturers and consumers because it is contributing to solving the time-consuming charging process and

short cruising range of electric vehicles (EVs) in the case of dynamic WPT [1-3]. However, in the WPT system, the phenomena of vertical offset and horizontal offset between the primary coil and the secondary coil are inevitable, resulting in a decrease in the output power and transmission efficiency. The coupling coefficient between the two coils is a vital factor that influences the output power and system transmission efficiency. In order to improve the coupling coefficient, an optimization topology of the WPT system was proposed in [4, 5] and different shapes of the coil were designed and the ferrite cores were added to the coils in [6, 7]. However, one can not ignore the problems of electromagnetic environment radiation and safety issues for the human body especially for important organs with the WPT system. When the electromagnetic radiation in the biological activity area exceeds the standard for safety levels with respect to human exposure to electric and magnetic fields, biological safety will be threatened. Therefore, it is necessary to study electromagnetic radiation and safety issues in the WPT system. In this paper, the EV model and the human body with five important organs were established to evaluate electromagnetic environment safety. In addition, the influence of ferrite cores on coupling coefficient and magnetic induction is analyzed and compared. Then the shielding effect using aluminum plates is studied on the electromagnetic radiation.

2 Mathematical model analysis

2.1 Wireless power transfer system

A WPT system can be divided into two main parts:the magnetic coupling mechanism and the power electronics system, which is shown in Fig.1. The magnetic coupling mechanism is made of a primary coil (under the ground) and a secondary coil (installed on the chassis of an Electric Vehicle). The Direct Current (DC) from the power supply is converted to Alternating Current (AC) with high frequency by the power electronics inverter. The power is then transmitted from the primary coil to the secondary coil through the electromagnetic field, using the AC/DC rectifier and energy management system to charge the battery.

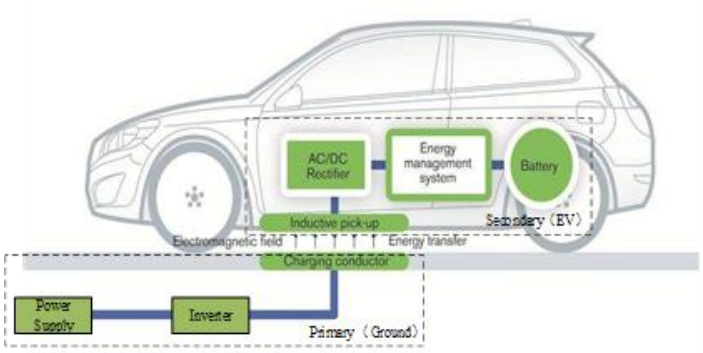

Figure1: A WPT system diagram of an electric vehicle

2.2 WPT system model

An equivalent circuit model of a WPT system with compensation capacitors arranged in an SS topology is shown in Fig. 2. For simplification, the equivalent source resistance is neglected. Here, the subscripts “1” and “2” refer to the “primary” and “secondary” coil values of inductor L, resistance R, and capacitance C, respectively. V_1 is the fundamental sinusoidal component of the source voltage of the primary circuit. R_L is the equivalent load resistance of the secondary side AC/DC converter. I_1 is the source current flowing through the primary coil, and I_2 is the load current flowing through the secondary coil.

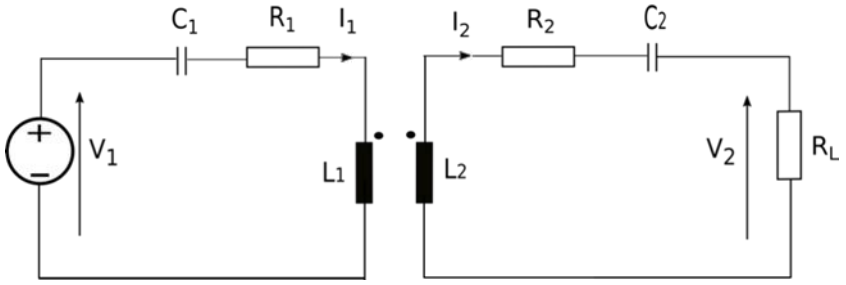

Figure2:Equivalent circuit model for SS topology [8].

The degree of the coupling between two coils can be expressed with the coupling coefficient k, which has a value ranging from 0 to 1, and is defined by Eq. (1). M represents the mutual inductance between primary and secondary coils.

$$k = \frac{M}{\sqrt{L_1 * L_2}} \tag{1}$$

The voltage equations in Fig. 2. can be written using the mutual inductance, M. ω is the frequency of V1.

$$\begin{aligned} \underline{V}_1 &= \left(\frac{1}{j\omega C_1} + j\omega L_1 + R_1\right)\underline{I}_1 - j\omega M\underline{I}_2 \\ \underline{V}_1 &= \left(\frac{1}{j\omega C_1} + j\omega L_1 + R_1\right)\underline{I}_1 - j\omega M\underline{I}_2 \end{aligned} \tag{2}$$

The resonance frequencies ω_0 at the primary coil and the secondary coil are assumed to be equal to

$$\omega_0 = \frac{1}{\sqrt{L_2 * C_2}} = \frac{1}{\sqrt{L_1 * C_1}} \tag{3}$$

At the resonance frequency ω_0, Eq. (2) can be rewritten as Eq. (4).

$$\begin{aligned} \underline{V}_1 &= R_1\underline{I}_1 - j\omega_0 M\underline{I}_2 \\ V_2 &= j\omega_0 M\underline{I}_1 - R_2\underline{I}_2 \end{aligned} \tag{4}$$

In Fig. 2, the delivered power to the load P_L, and the transfer efficiency η at the resonant frequency ω_0, can be obtained as follows in Eq. (5) and Eq. (6) .

$$P_L = \frac{\omega_0^2 M^2 \underline{V}_1^2 R_L}{[R_1(R_L + R_2) + \omega_0^2 M^2]^2} \tag{5}$$

$$\eta = \frac{\omega_0^2 M^2 R_L}{R_1(R_L + R_2)^2 + \omega_0^2 M^2 (R_L + R_2)} \tag{6}$$

2.3 Principle of the numerical method

The finite element method, whose principle is to solve Maxwell equations under given boundary conditions, is used to analyze the electromagnetic field of the WPT system. The differential forms of Maxwell equations from Eq. (7) to Eq. (10) are shown as follows.

$$\nabla \times H = J + \frac{\partial D}{\partial t} \tag{7}$$

$$\nabla \times E = -\frac{\partial B}{\partial t} \tag{8}$$

$$\nabla \cdot D = \rho \tag{9}$$

$$\nabla \cdot B = 0 \tag{10}$$

When applying Maxwell equations, it is necessary to consider the influence of the medium on the electromagnetic field. In a uniform isotropic medium, the relationships between the physical quantities of the electromagnetic field and the characteristic quantities of the medium are calculated by Eq. (11), Eq. (12), and Eq. (13) below.

$$B = \mu H \tag{11}$$

$$D = \varepsilon_0 \varepsilon_r E \tag{12}$$

$$J = \sigma E \tag{13}$$

Where H is the magnetic field intensity (A/m), J is the current density (A/m^2), D is the electric flux density (C/m^2), E is the electric field intensity (V/m), B is the magnetic induction intensity (T), ρ is the charge density (C/m^3), μ is the magnetic permeability (H/m), ε_0 is the dielectric constant of vacuum (F/m), the value is 8.85×10^{-12} , ε_r is the dielectric permittivity, σ is the electric conductivity (S/m). Maxwell equations provide a theoretical basis for simulating the electromagnetic field environment by COMSOL.

3 Modeling and design of magnetic coils, human body model and organs in WPT systems

The magnetic coupling structure is a vital factor affecting the transmission power and efficiency of a WPT system. A typical magnetic coupling system is composed of three components: coils, ferrite cores, and aluminum shielding. In this system, the coil is made of isolated Litz wire. The ferrite core is made of ferromagnetic materials, and the shielding part is made of conducting materials. Because of the low coupling coefficient between transmitting and receiving coils, the ferrite cores are usually used to improve coupling ability and transmission efficiency. However, ferrite cores will also improve magnetic induction intensity and increase the stray field around the coil, which will threaten biological safety. Therefore, the aluminum shielding is added to the ferrite cores with coils.

3.1 WPT magnetic coil model

The WPT system typical coil shapes include circular, square, rectangular and double D (DD) coil configurations. The circular coil is studied and shown that it has a high coupling coefficient when the misalignment is small [9]. Therefore, the circular coil is modeled by the 3D FEM software COMSOL to compare magnetic field distributions under different models of only coils, coils with ferrite cores, and coils

with ferrites and aluminum plates. The different magnetic coil models are presented in Fig. 3. The parameters of the circular coil, ferrite cores and aluminum plate are listed in Table 1. During the simulation, the parameters of the primary coil and secondary coil are set as the same value. The air-gap distance is fixed at 180 mm.

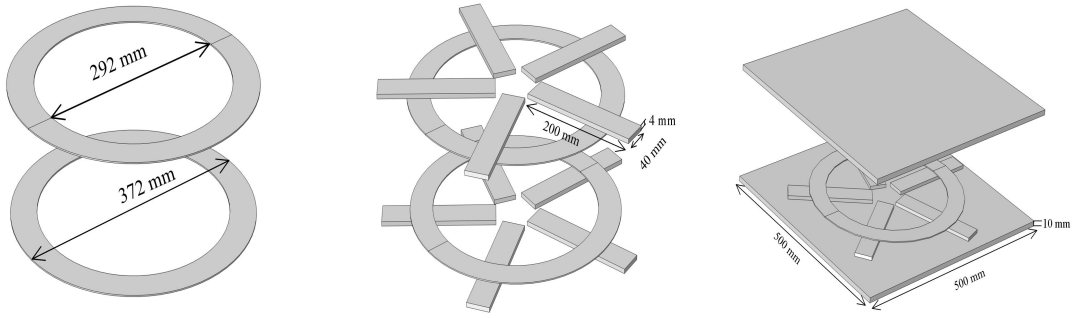

(a) (b) (c)

Figure3: Magnetic coil models. (a) Only coils. (b) Coils with ferrite cores.(c) Coils with ferrite cores and aluminum plates.

Table1: Parameters of the circular coils, the ferrite cores and the aluminum plates.

Symbol	Quantity	Value
R_i	inner hole radius	146 mm
R_o	outer radius	186 mm
N	the number of the coil turns	22
S	wire cross-sectional area	2.6 mm^2
a×b×t	dimension of ferrite core	200 mm x 40 mm x 7 mm
u_r	relative magnetic permeability	800
c×d×h	dimension of aluminum plate	500 mm x 500 mm x 10 mm

3.2 Simulation results of magnetic coil model

In this part, the magnetic field distributions are analyzed by COMSOL based on the impact on only coils, coils with ferrite cores and coils with ferrite cores and aluminum plates. The simulation results are shown in Fig. 4.

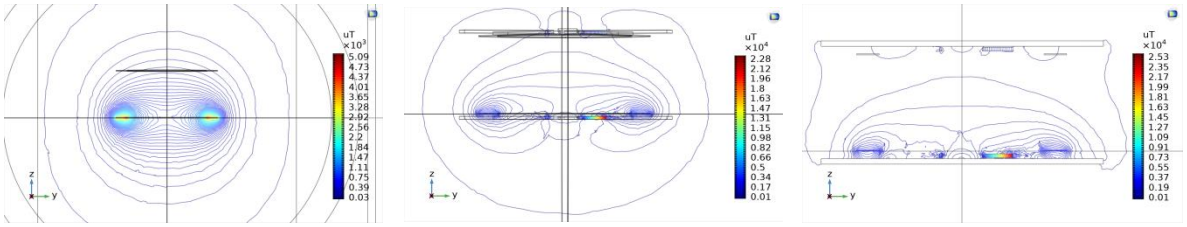

(a) (b) (c)

Figure4: Magnetic field distributions. (a) Only coils. (b) Coils with ferrite cores. (c) Coils with ferrite cores and aluminum plates.

From the above simulation results, it can be concluded that the magnetic field induction is mainly concentrated between the two coils with additional ferrite cores, which is beneficial to improve the coupling coefficient. However, it may lead to the coil magnetic field exceeding the standard for safety levels regarding human exposure magnetic field induction. Therefore, two aluminum plates are placed on the primary and secondary sides in Fig. 4 (c), which indicates that aluminum plates can effectively reduce the diffusion of the magnetic field to the surrounding.

3.3 EV model

To make the simulation software COMSOL calculation fast and accurately, and the grid breakage is simple, the EV model is simplified and then built using SolidWorks. According to the typical size of the electric vehicle model, the length, width and height of this EV model are 4110 mm,1590 mm,1517 mm in Fig.5.

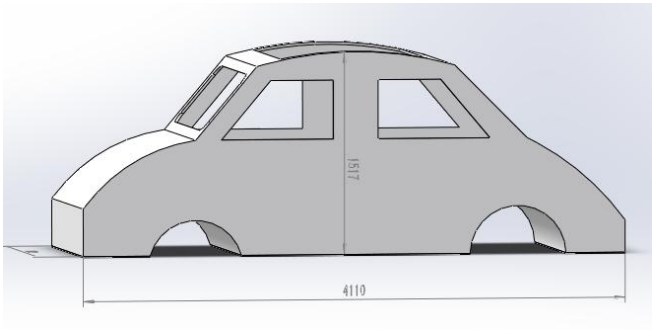

Figure5: The diagram of the EV model.

3.4 Human body model in different postures

To anlyze the influence of the electromagnetic fields on the human body, a 3D human body model is established in Fig. 6. According to the Human Engineering for Chinese people, the standing and sitting model's height is set to 177.5 cm and 125.3 mm, respectively. In the literature [10], the relative permeability of the human body model is 3100, the electrical conductivity sets to 0.129 S/m, and human body density is 1033 kg/m^3. The sitting human body model is used to study the magnetic exposure of an adult sitting in the drive's seat, while the standing human body model is used to explore the magnetic exposure of an adult standing near the WPT coils around the EV.

There are four measurement points, which represent one adult's foot (A), leg (B), chest (C) and head (D) are illustrated in Fig. 6. In Fig 6 (a), the secondary coil is placed under the driver's seat and the distance from the foot to the chassis of the EV is 10 cm. In Fig.6 (b), the distance between the measurement point and the y-axis is 70 cm. Moreover, the position of the primary coil and the secondary coil is kept in the same position. In addition, the air gap between the primary and secondary coil is set to 18 cm, and the primary coil is embedded under the ground. The standard of the International Commission on Non-Ionizing Radiation Protection (ICNIRP) is used to limit human exposure to electromagnetic fields.

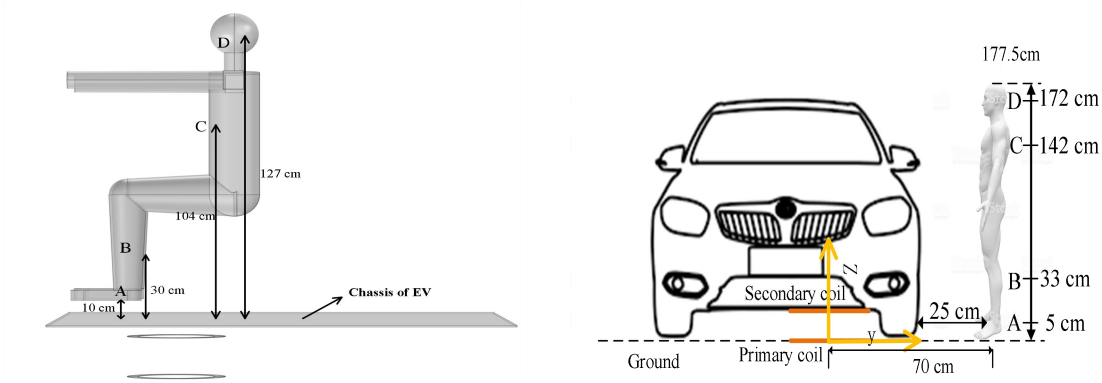

(a) (b)

Figure6: An adult body model in different postures in the WPT system. (a) an adult body model sitting in the driver's seat. (b) an adult body model standing around the EV.

Based on the EV model and human body model, the position of the important human organs is designed including the feet, liver, spleen, heart, lung and kidney. Table 2 shows the Electromagnetic parameters of the six organs.

Table2: Electromagnetic parameters of the human body at the frequency 85 kHz.

Organs	Relative permittivity	Conductivity (s/m)
feet	3100	0.129
liver	10120	0.08848
spleen	5022	0.1098
heart	14350	0.74
lung	3025	0.3
kidney	10019	0.2018

In order to simplify the calculation, only the chassis of the EV model is retained, and other parts are removed in the simulation. Moreover, the human body is divided into different parts according to the needs of the analysis and the material of the chassis is steel.

4 Analysis and simulation results

4.1 Electromagnetic safety standards

Table 3 shows the public exposure control limit values at 85 kHz, including the standard of Electrical and Electronics Engineers (IEEE) [11], the International Commission on Non-Ionizing Radiation Protection (ICNIRP) [12] and Chinese Standard GB/T 38775.4-2020 In this study, the standard of ICNIRP is used to limit human exposure to electromagnetic fields.

Table3:The standard for safety levels for human exposure of electric and magnetic fields at the frequency 85 kHz.

Standard	Magnetic flux density	Electric fields (V/m)
ICNIRP	27	83
IEEE	205	614
GB/T 38775.4-2020	27	83

4.2 Simulation results of the magnetic flux density in different postures

Considering the influence of different magnetic coupling mechanisms and can metal body on the electromagnetic field, this section discusses the electromagnetic field distribution in the human body when the adult is sitting in the car and standing near the charging coil outside the car. In this section, the cases of the circular coil with or without ferrite cores and aluminum plate are analyzed. Moreover, the magnetic flux density of the human body mode under the different scenarios with a car metal body is analyzed, which is illustrated in Fig. 7 and Fig. 8.

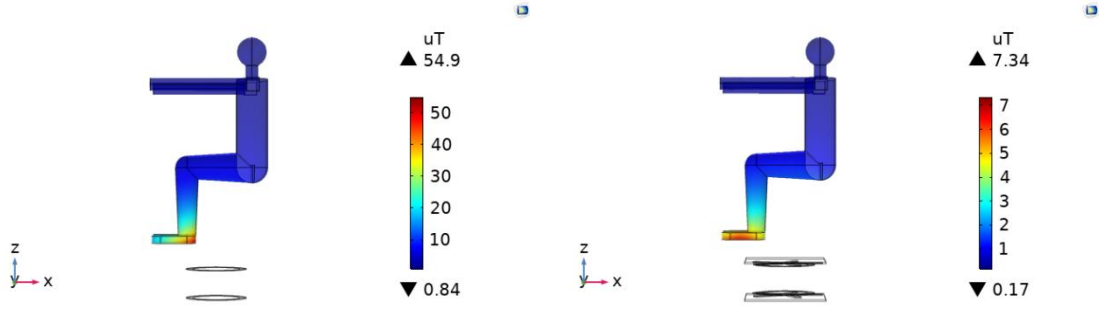

(a) (b)

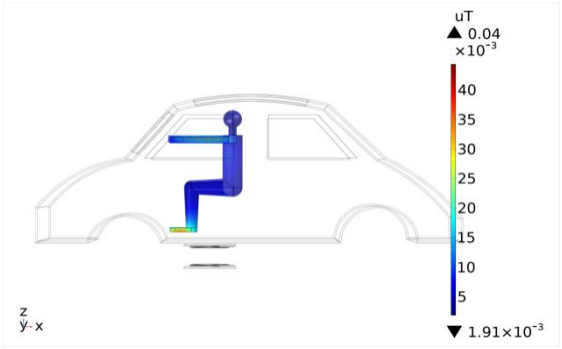

(c)

Figure7: The magnetic flux density in the adult sitting model: (a) Only coils; (b) Coil with ferrite cores and aluminum plates; (c) Coil with ferrite cores, aluminum plate and car metal body.

Fig. 7 shows the magnetic flux density of a sitting human body model when only circular coils, coils with ferrite cores and aluminum plate, and car metal body are added to the model. The simulation results prove that the ferrite core and aluminum plate can effectively reduce the sitting human's magnetic flux density in the WPT system. In the coils with ferrite cores and aluminum plate, the maximum magnetic flux density is 7.34 uT,

which is 86.63% reduction compared with 54.9 uT when only coils are used. However, the maximum magnetic flux density is only 0.04 uT when the car metal body is added.

The standing human body model with a metal car body, the ferrite cores and the aluminum plate is similar to the sitting human body in Fig. 8. The ferrite core and aluminum plate have a certain shielding effect on the electromagnetic field and protect the human body. Compared with only the coils, in the coils with ferrite cores and aluminum plate, the maximum magnetic flux density is reduced from 23.8 uT to 7.91 uT, a 66.76% reduction. Compared with the human sitting outside the car, the protective effect of the ferrite cores and aluminum plate on the human body standing next to the coil is reduced. Therefore, each case's magnetic flux density is far less than the limit value specified in the ICNIRP guideline.

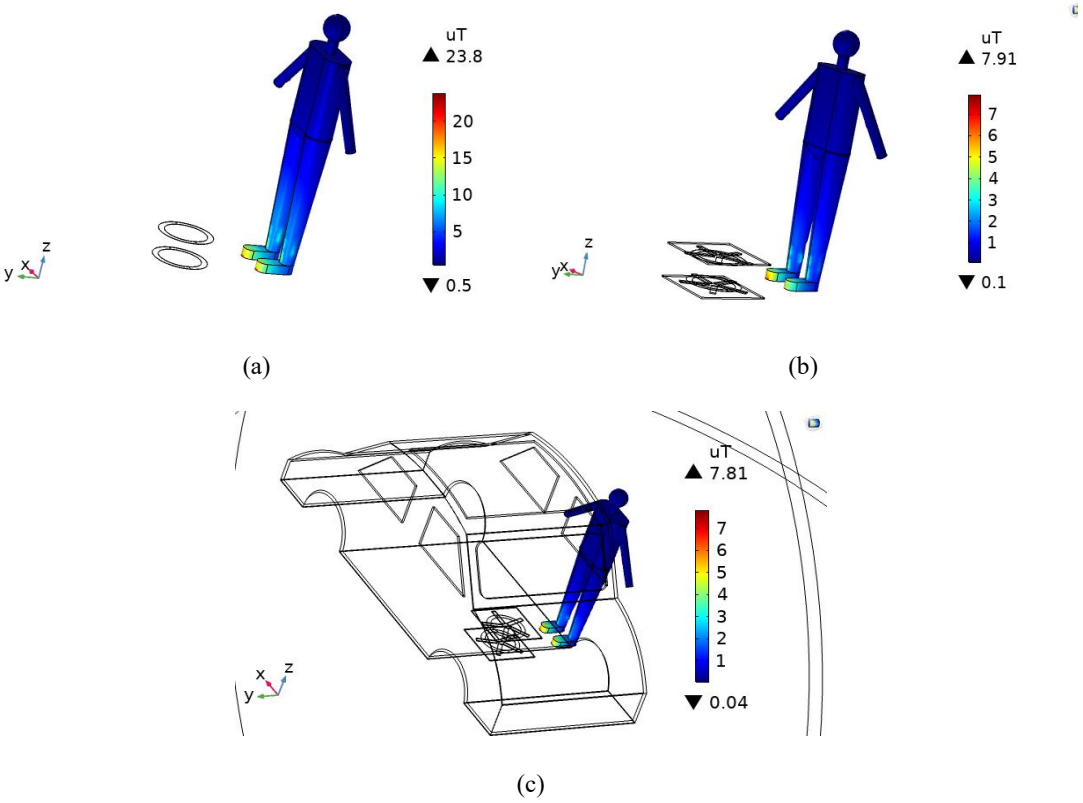

(a) (b)

(c)

Figure8: The magnetic flux density in the adult standing model: (a) Only coils; (b) Coil with ferrite cores and aluminum plates; (c) Coil with ferrite cores, aluminum plate and car metal body.

To further study the magnetic flux density of the adult model in different locations, four different body parts are chosen to get corresponding values using COMSOL. The magnetic induction intensity of the four body parts in the adult model is shown in Table 4.

Table4: Magnetic induction intensity of four body parts in the adult model (uT).

Body parts	Only coils		Coil with ferrite cores and aluminum		Coil with ferrite cores, aluminum plate and car metal body	
	sitting	standing	sitting	standing	sitting	standing
foot	110.61	46.15	7.71	13.71	0.051	14.62
leg	17.51	5.16	2.8	1.29	0.0092	1.1
chest	1.89	1.02	0.39	0.21	0.0038	0.073
head	1.12	0.59	0.23	0.12	0.0038	0.048

From the simulation results in Table 4 it can be seen that the magnetic flux density is up to 110.61 uT at the part representing the foot without considering the car metal body and the aluminum plate. It is three times more than the ICNIRP standard 27 uT. It can be concluded that it is essential to pay attention to the magnetic field shielding in designing the WPT system. Moreover, by comparing the simulation results for the sitting body and standing body with the car metal body, it is revealed since the metal car body itself has a shielding effect, the magnetic induction intensity in the car is small, so it is more important to suppress electromagnetic radiation around the body. Besides, it is urgent to pay more attention to electromagnetic protection on the feet.

4.3 Simulation results of the electric field density in different postures

As a similar analysis in the Section 4.3, the electric field distribution in the human body when the adult is sitting in the car and standing near the charging coil outside the car is discussed and analyzed in this part. In this section, the impact of different magnetic coupling mechanisms, including the only circular coil , the circular coil with ferrite cores and aluminum plate, and car metal body on the electric fields are considered. At the same time, the electric field density under the different scenarios with a car metal body is analyzed, which is illustrated in Fig. 9 and Fig. 10.

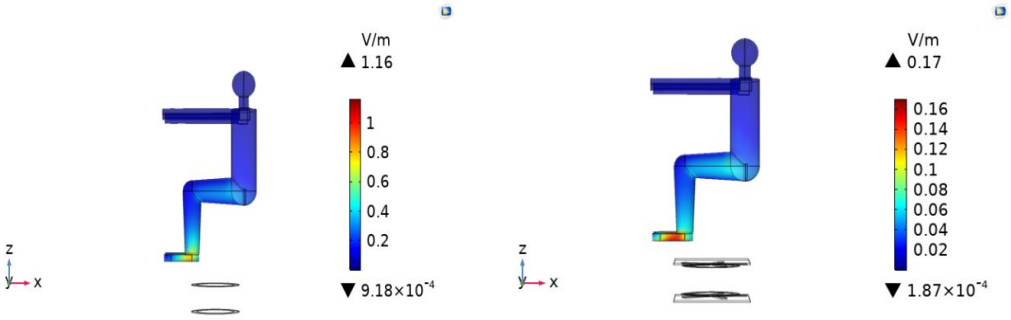

(a) (b)

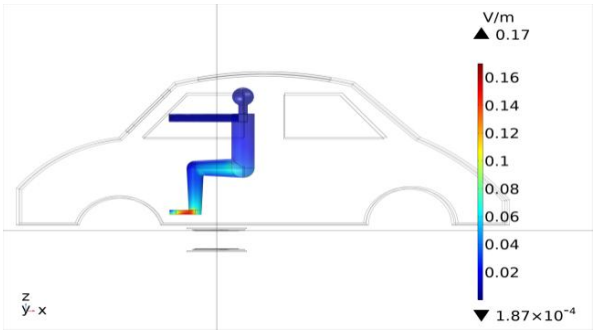

(c)

Figure9: The electric field density in the adult sitting model: (a) Only coils; (b) Coil with ferrite cores and aluminum plates; (c) Coil with ferrite cores, aluminum plate and car metal body.

The electric field density of a sitting human body under the condition of the circular coil with or without ferrite cores, aluminum plate and car metal body is presented in Fig. 9. From the simulation results, the electric field density is all small in all scenarios, even if the maximum electric field density of the adult sitting model with only coils is only 1.16 V/m, which is far less than the standard of ICNIRP, 83 V/m.

A similar study is carried out on the standing human model under the different scenarios of only magnetic coils, coil with ferrite cores and aluminum plate, and a metal car body, shown in Fig. 10, respectively. From the simulation results, it can be seen that the electric field density under the different scenarios is all small when an adult stands around the car.

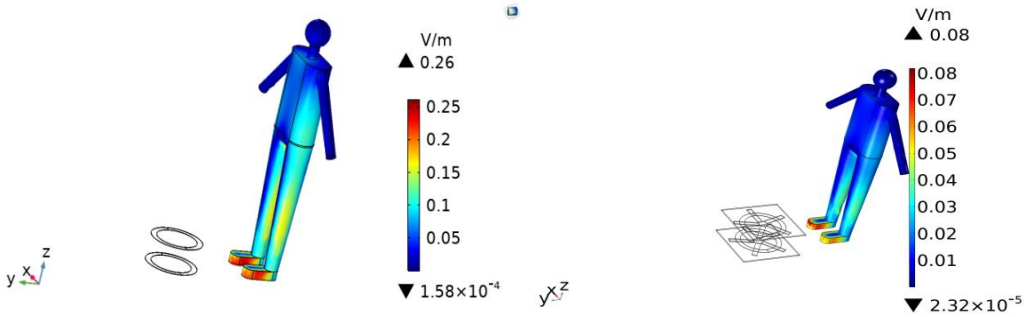

(a) (b)

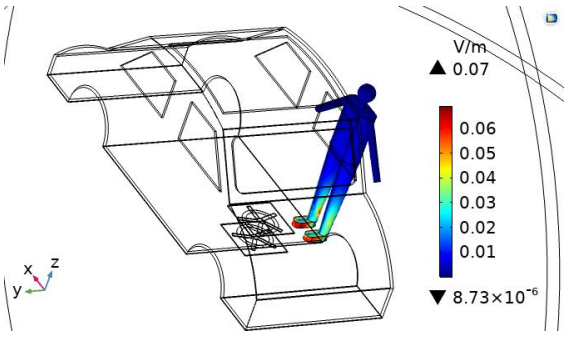

(c)

Figure10: The electric field density in the adult standing model: (a) Only coils; (b) Coil with ferrite cores and aluminum plates; (c) Coil with ferrite cores, aluminum plate and car metal body.

To further study the electric field density of the adult model in different locations, four different body parts are chosen to get corresponding values by COMSOL. The electric field density of the four body parts in the adult model is shown in Table 5.

Table5: Electric field intensity of four body parts in the adult model (V/m).

Body parts	Only coils		Coil with ferrite cores and aluminum		Coil with ferrite cores, aluminum plate and car metal body	
	sitting	standing	sitting	standing	sitting	standing
foot	1.53	0.26	0.22	0.078	0.0011	0.074
leg	0.155	0.032	0.021	0.079	0.000079	0.006
chest	0.044	0.03	0.0083	0.0062	0.00008	0.0013
head	0.045	0.01	0.0068	0.0021	0.00024	0.00081

From the simulation results in Table 5, it can be seen that the maximum value reach 1.53 V/m, which is far less than the value specified in the ICNIRP guideline, 87 V/m. Compared with the simulation of magnetic flux density, it can be concluded that in the electromagnetic safety of a WPT system, it should pay more attention to the magnetic field exposure on the human body.

4.4 Simulation results of the magnetic flux density and electric field in human body organs

The study of section 4.3 proves that people standing outside the car are more exposed to electromagnetic radiation and human body is more exposed to magnetic field radiation. Fig.11 and Fig.12 show the magnetic flux and electric field strength distribution of the human organs under the condition of only coils, coils with ferrite bars and coils with ferrite bars and aluminum plates, respectively.

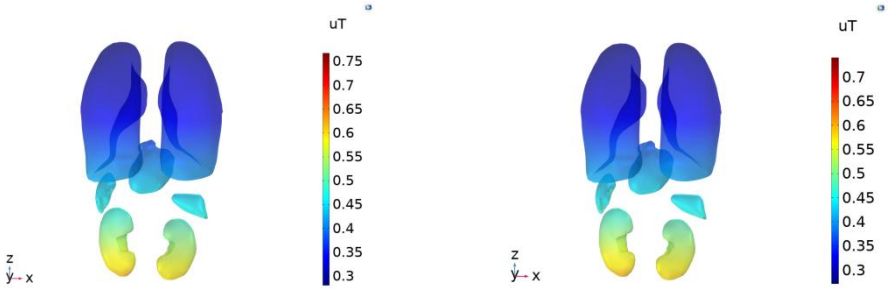

(a) (b)

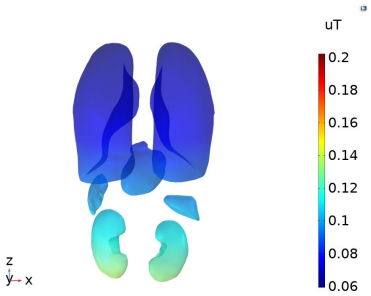

(c)

Figure11: Magnetic flux distribution of other organs. (a) Only coils. (b) Coils with ferrite cores. (c) Coils with ferrite cores and aluminum plates.

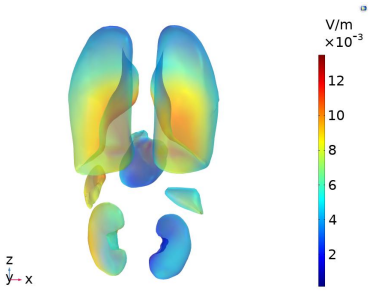

(a)

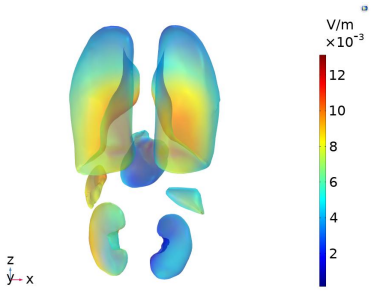

(b)

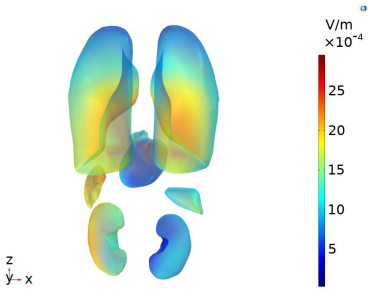

(c)

Figure12: Electric field strength of other organs. (a) Only coils. (b) Coils with ferrite cores. (c) Coils with ferrite cores and aluminum plates.

Table 6 and Table 7 show the maximum value of magnetic induction density and electric field intensity of each human body organs, respectively.

Table 6: The maximum value of magnetic induction density (uT) for human body parts at the frequency 85 kHz.

Organs	Only coils	Coils with ferrite	Coils with ferrite cores and aluminum
liver	0.77	0.5	0.21
spleen	0.16	0.62	0.1
heart	0.46	0.44	0.0001
Lung	0.42	0.41	0.0009
kidney	0.67	0.72	0.14

Table 7: The maximum value of electric field strength (V/m) for human body parts at the frequency 85 kHz.

Organs	Only coils	Coils with ferrite cores	Coils with ferrite cores and aluminum plates
liver	0.0079	0.0077	0.0017
spleen	0.0127	0.0124	0.0027
heart	0.0113	0.011	0.0024
Lung	0.0137	0.0133	0.003
kidney	0.0121	0.012	0.0027

From the Table 6 and Table 7, it can be concluded that the electromagnetic radiation intensity received by the internal organs of the human body is relatively small because of the protective effect of human skin. The addition of aluminum plates is beneficial to reduce the electromagnetic radiation received by the organs.

5 Conclusion

The results show that the electromagnetic safety indexes at most scenarios meet the ICNIRP standard for different cases, except for the situation the magnetic flux density of a sitting human body without a metal body exceeded the standard of ICNIRP. Also, the magnetic core and aluminum plate can significantly reduce human body exposure to the magnetic field. The aluminum plate has been confirmed to have a certain shielding effect on magnetic radiation. The final results also illustrate that the electromagnetic field and the induced electric field exposure of the human sitting in the car can be reduced due to the magnetic shielding effect of the metal car body, so the metal car body can make humans sitting in the car safer. As for the human standing next to the coils, the metal car body has the opposite effect. In general, the electromagnetic environment of wireless charging for electric vehicles is safe for the human body. Finally, some essential human organs for the human body is established, including liver, spleen, heart, lung and kidney. Furthermore, the five important organs were simulated in different scenarios with only coils, the coils with ferrite cores and the coils with ferrite cores and aluminum plates. The simulation results show that the electromagnetic safety indexes of each organ all meet the ICNIRP standard for different cases.

Acknowledgments

This work was supported by the National Key Research and Development Program of China (2021YFB1600200), the Natural Science Foundation of Shaanxi Province (2020JQ-385), the Fundamental Research Funds for the Central Universities, CHD (300102222202), and Open Project of Key Laboratory of Solar Energy Utilization & Energy Saving Technology of Zhejiang Province (ZJS-OP-2020-08).

References

[1] L. Yang, B. Zhang and M. Ju, "A Fast Dynamic Response Regulation Method for Undersea Wireless Power Transfer System," 2019 14th IEEE Conference on Industrial Electronics and Applications (ICIEA), Xi'an, China, 2019, pp. 1162-1166.

[2] I. Suh and J. Kim, "Electric vehicle on-road dynamic charging system with wireless power transfer technology," 2013 International Electric Machines & Drives Conference, Chicago, IL, 2013, pp. 234-240.

[3] M. Debbou and F. Colet, "Inductive wireless power transfer for electric vehicle dynamic charging," 2016 IEEE PELS Workshop on Emerging Technologies: Wireless Power Transfer (WoW), Knoxville, TN, 2016, pp. 118-122.

[4] W. Zhang and C. C. Mi, "Compensation Topologies of High-Power Wireless Power Transfer Systems," in IEEE Transactions on Vehicular Technology, vol. 65, no. 6, pp. 4768-4778, June 2016.

[5] R. Mai, Y. Chen, Y. Zhang, N. Yang, G. Cao and Z. He, "Optimization of the Passive Components for an S-LCC Topology-Based WPT System for Charging Massive Electric Bicycles," in IEEE Transactions on Industrial Electronics, vol. 65, no. 7, pp. 5497-5508, July 2018.FLEXChip Signal Processor (MC68175/D), Motorola, 1996.

[6] Nagendra, G.R.; Covic, G.A.; Boys, J.T. Determining the Physical Size of Inductive Couplers for IPT EV Systems. IEEE J. Emerg. Sel. Top. Power Electron. 2014, 2, 571 – 583.

[7] T. Kim, S. Yoon, J. Yook, G. Yun and W. Y. Lee, "Evaluation of power transfer efficiency with ferrite sheets in WPT system," 2017 IEEE Wireless Power Transfer Conference (WPTC), Taipei, 2017, pp. 1-4.

[8] Yang, Y., Baghdadi, M. El., Lan, Y., Benomar, Y., et al.,2018. Design Methodology, Modeling, and Comparative Study of Wireless Power Transfer Systems for Electric Vehicles. Energies, 11(7), 1716.

[9] Yang, Y., Cui, J., Cui, X., 2020.Design and analysis of magnetic coils for optimizing the coupling coefficient in an electric vehicle wireless power transfer system. Energies 13(16).

[10] Dong, Y., Wang, L., Lyu, J., et al.,2018.Electromagnetic safety simulation analysis of electric ambulance wireless charging system.Chinese Medical Equipment 39(8),1-5.

[11] Li Siqi, Mi Chcric. Wireless power transfer for electric vehicle applications[J]. IEEE Journal of Emerging and Selected Topics in Power Electronics, 2015, 3(1): 4-17.

[12] Guidelines for limiting exposure to time-varying electric and magnetic fields (1Hz to 100kHz)[J]. Health Physics, 2010, 99(6): 818-836.

Authors

Dr. Yang Yang is currently an associate professor in School of Automobile, Chang'an University. He received the M.S. degree in Electrical Engineering from Northwestern Polytechnical University (NPU) and a Ph.D. degree in inductive power transfer charging system for electric vehicles from Vrije Universiteit Brussel (VUB), Belgium in 2013 and 2018, respectively. His research interests include wireless power transfer, power electronic technology, and on-road charging for electric vehicles.